Hydrometallurgy 182 (2018) 128–135

Contents lists available at ScienceDirect

Hydrometallurgy

journal homepage: www.elsevier.com/locate/hydromet

Interactions of mimic weathered pyrite surfaces (FeS_2) with acidic culture media (0 K): An approach for (bio)leaching applications

Albert Saavedra[a], J. Viridiana García-Meza[b], Eduardo Cortón[a], Ignacio González[c,*]

[a] Biosensors and Bioanalysis Laboratory (LABB), Departamento de Química Biológica and IQUIBICEN-CONICET, Facultad de Ciencias Exactas y Naturales, Ciudad Universitaria, Universidad de Buenos Aires (UBA), Pabellón 2, Ciudad Autónoma de Buenos Aires, Argentina
[b] Geomicrobiología, Facultad de Ingeniería-Metalurgia, UASLP, Sierra Leona 550, Lomas, San Luis Potosí 278210, Mexico
[c] Departamento de Química, Universidad Autónoma Metropolitana-Iztapalapa, Av. San Rafael Atlixco No. 186, Col. Vicentina, Ciudad de México 09340, Mexico

ARTICLE INFO

Keywords:
Bacterial attachment
Interfacial modifications
Mineral-culture media interaction
Pyrite oxidation
Pyrite weathering
Raman spectroscopy

ABSTRACT

In biohydrometallurgical processes, a mineral exhibits different oxidation phases due to the system's heterogeneity, especially in heap leach pads. Oxidation chemically modifies the mineral surface altering its interface, and thereby affecting the bacteria-mineral interaction, mineral reactivity and leaching velocity. Given that the mineral can be found in different oxidation states in heap bioleaching processes, three oxidation conditions of FeS_2, in which iron and/or sulfur related compounds are formed on the mineral surface were assayed. This paper studies the interaction between the modified surface of a sulfide mineral, FeS_2, and 0 K culture medium, typically used in biomining processes. Chemical and electrochemical changes on surfaces were characterized by subjecting them to weathering in an acidic culture medium (pH 1.8), without applying potential or current. The chemical species formed were identified by Raman spectroscopy. The modified pyrite surfaces showed significant interfacial transformations upon immersion in the culture medium, and the formation of passive chemical species, such as elemental sulfur, jarosite, phosphates and oxides, were identified. These interfacial modifications are correlated with changes in the open circuit potential (OCP) values during immersion of pyrite and surface modified pyrites in 0 K culture medium. Electrochemical characterization showed a decrease in mineral oxidation capacity, which directly affects the extent of leaching and possibly, of the interaction with other elements participating in the process, such as microorganisms. To study the interactions among bacteria and the pyrite mineral suffering different surface modifications, the attachment of the bioleaching bacterium Leptospirillum sp. was evaluated.

1. Introduction

In the past decades, the use of alternative technologies has been implemented in low-grade sulfide mineral processing. One of these technologies is biohydrometallurgy, process where metal solubilization from sulfide ores is mediated by microorganisms (Vera et al., 2013). During the leaching process, the mineral exhibits different oxidation phases due to the heterogeneity of the system, especially in heap leach pads (Lara et al., 2015; Xia et al., 2010; Yang et al., 2015). Oxidation chemically modifies the mineral surface altering its interface, and thereby affecting the bacteria-mineral interaction, mineral reactivity and leaching velocity (Lara et al., 2015; Lázaro et al., 1997).

Particularly in biohydrometallurgical processes, the mineral is in contact with acidic culture media containing anions and cations necessary for microbial metabolism (Jones and Kelly, 2008). Microorganisms that usually participate in these processes have chemolitotrophic metabolism, that is, their sources of carbon and energy are of inorganic origin (Rohwerder et al., 2003). Such is the case of *Acidithiobacillus ferrooxidans*, whose source of carbon from CO_2 fixation and the source of energy, from iron and sulfur oxidation (Tuovinen and Kelly, 1973). Besides, microorganisms require other chemical components to synthesize their basic products in order to subsist, and they have to be contained in the leaching solution. These elements are usually found in culture media in the form of ammonium salts, phosphates and sulfates (Tuovinen and Kelly, 1973). They may interact with the mineral and change its surface and characteristics (Cruz et al., 1997), resulting in the formation of passive compounds of sulfur, iron oxides, and $FePO_{4(S)}$ precipitates on pyrite (FeS_2) and chalcopyrite ($CuFeS_2$) in the culture medium (Lara et al., 2015). There are a very few studies that characterize this phenomenon, which can be important in bacteria-mineral interaction phenomena (Cruz et al., 2005; Florian et al., 2011), as well as in industrial bioleaching (Watling, 2006), and

* Corresponding author.
E-mail address: igm@xanum.uam.mx (I. González).

https://doi.org/10.1016/j.hydromet.2018.10.022
Received 21 April 2018; Received in revised form 9 October 2018; Accepted 26 October 2018
Available online 07 November 2018
0304-386X/

bio-oxidation processes (Acevedo et al., 1998).

During manipulation and weathering, the mineral undergoes different chemical surface transformations forming iron- and/or sulfur-based products. When these are put in contact with the culture medium, they can undergo even more significant changes because oxidizing conditions vary with depth, depending on environmental conditions of the process (T°, pH, dissolved O_2, etc.) (Murr and Brierly, 1978; Davis and Ritchie, 1986; Zhang and Liu, 2017). These surface changes can modify the open circuit potential (OCP) and the mineral surface tension (Fredlein et al., 1971; Marshall, 1986), and be important for improving bacteria-mineral interaction (Cruz et al., 2005); however, in other cases, they can cause opposite results, such as formation of passive products (Lara et al., 2015). The interaction between *A. ferrooxidans* and arsenopyrite was previously characterized by our research team, where the presence of realgar (As_2S_2), formed by the spontaneous chemical reaction between arsenopyrite and the culture medium proved to prevent bacterial adhesion, diminishing the extent of bio-leaching (Cruz et al., 2005; Lázaro and González, 1997).

Bacteria-mineral interactions are relevant to bio-leaching process. If well sometimes a denominated 'direct mechanism' (where lixiviation proceeds by bacterial attachment) has been proposed, nowadays the 'indirect mechanism' is considered the most probable mechanism, where the microorganism's most relevant function is to catalyze the production of ferric ion, a strong oxidizing agent. The microorganisms may perform this process either in the planktonic or sessile form (biolfilm). Biofilm production can accelerate the bio-leaching by accumulating higher concentration of ferric ion (with respect to the surrounding solution) in the extracellular polymeric substances (EPS). The attachment of bacteria to the mineral is the first step of biofilm establishment, and so relevant to biomining process (Vera et al., 2013; Saavedra et al., 2018).

The surface state of pyrite was chemically modified to mimic surface modifications that might be present in different areas of heap leach pads or during mineral processing. Chemical treatments consisted specifically in modifying surfaces of pyrite electrodes with iron and sulfur related compounds (FeS_2/$Fe(OH)_n$,S^0), iron related compounds (FeS_2/$Fe(OH)_n$) and sulfur related compounds (FeS_2/S^0); a pyrite electrode (FeS_2) was used as control.

This study correlates chemical alterations occurring in pyrite and modified pyrite electrodes from the electrochemical and chemical points of view, by mimicking different oxidation states of the minerals exposed to an abiotic culture medium. Raman spectroscopy was used to identify chemical compounds formed on mineral surfaces due to the reaction with the culture medium, and their reactivity and oxidation capacity were evaluated by electrochemical techniques. Para estudiar la importancia en la interacción bacteria-mineral, se evaluó la adherencia de la bacteria biolixiviante *Leptospirillum* sp. sobre estos minerales de pirita. The interaction bacteria-mineral was studied by means of the well-know bioleaching bacteria, Leptospirillum sp.; to that end, adherence experiments to pyrite and surface-modified pyrite were performed.

2. Material and methods

2.1. Mineral

Pyrite samples were obtained from Navajun (Spain). Mineral identity and composition were verified by X-ray diffraction patterns (XRD, Rigaku 22,002, Θ = 0.02, 10 to 90°, using Cu-Kα radiation) and scanning electron microscopy (SEM, Philips XL30) coupled with an energy dispersive Si(Li) detector (EDAX DX4) (Fig. S1). Prior to XRD analysis, the samples were pulverized in an agate mortar. Pyrite with 61.82% *w*/w purity additionally contains nacrite ($Al_2(Si_2O_5)(OH)_4$, 38.18% *w*/w).

2.2. Electrochemical cell and electrodes

A typical 50-mL three-electrode electrochemical cell was used. A modified 0 K culture medium (Kim et al., 2002), supplemented with ($g\,L^{-1}$): KCl, 1.0; $MgSO_4{\cdot}7H_2O$, 0.2; $(NH_4)H_2PO_4$, 2.6, was used as electrolytic solution. The pH was adjusted to 1.8 with 10 N H_2SO_4. All the experiments performed in the electrochemical cell were performed in static conditions (without stirring or bubbling gases), and the temperature was maintained at 30 °C by using a thermostatic bath.

Mineral electrodes were constructed from the natural FeS_2 ore and were used as working electrodes (WEs). They were prepared from a massive sample mineral; samples were cut into cubic shapes and encapsulated in epoxy resin. The exposed electrode area was ca. 1.0 cm^2. Before each experiment, the WE exposed surface was renewed by polishing with sandpaper (1200#). A graphite bar (Alfa Aesar 99.999% purity) was used as counter electrode (CE). The reference electrode (RE) was a $Hg/HgSO_4/K_2SO_{4(sat)}$ (SSE; 0.640 V/NHE), immersed in a Luggin capillary. All potential values reported in this study refer to the normal hydrogen electrode (NHE).

2.3. Previous preparation of different pyrite surfaces (modified surfaces)

To mimic different stages of the mineral that can be found in mining processes, the surface state of pyrite was chemically modified. Chemical treatments consisted specifically in modifying surfaces of pyrite electrodes with the compounds related to: (1) iron and sulfur (FeS_2/$Fe(OH)_n$,S^0), (2) iron (FeS_2/$Fe(OH)_n$) and (3) sulfur (FeS_2/S^0); a pyrite electrode (FeS_2) was used as control.

To obtain pyrite modified with iron and sulfur related compounds (FeS_2/$Fe(OH)_n$,S^0), pyrite was subjected to chemical oxidation catalyzed by ferric ion in acidic medium (pH 1.8). Chemical oxidation was carried out by placing the electrode in a 250-mL Erlenmeyer flask containing ferric oxidizing solution under orbital stirring at 200 rpm and 30 °C during 7 days (Cruz et al., 1997). Ferric solution was prepared by oxidation of 2 g $FeSO_4{\cdot}7H_2O$ diluted in 100 mL of deionized water using H_2O_2. The 0.9 M H_2O_2 was added in stepwise fashion until reaching the minimum quantity required to oxidize the ferrous ion without any remainder in solution; iron oxidation was verified by monitoring oxidation-reduction potential (ORP).

On the other hand, to obtain pyrite electrodes with iron related compounds, sulfur was removed (from previously modified pyrite specimens) with a methanol wash (FeS_2/$Fe(OH)_n$); to do that, pyrite electrodes were stirred in a 250-mL Erlenmeyer flask containing 100 mL of methanol under stirred conditions, and following the method reported by several authors (Fernandez et al., 1995; McGuire and Hamers, 2000; Mustin et al., 1993; Cruz et al., 1997)

Lastly, to obtain a pyrite electrode with sulfur related compounds on its surface, the iron (from previously modified pyrite specimens) was removed using HCl (FeS_2/S^0); to do that pyrite electrodes were stirred in a 250-mL Erlenmeyer flask containing 100 mL of hydrochloric acid 5 N. Both methanol and HCl wash were performed under stirring at 200 rpm for 48 h at 30 °C (Cruz et al., 1997).

2.4. Raman spectroscopy analysis

Surface modified pyrite electrodes remained immersed in 0 K culture medium for 48 h to ensure the electrode stability after weathering. At 0 h and after 48 h of immersion, Raman spectra of each electrode were recorded, using a spectrometer (T64000 Jobin Yvon) coupled to a confocal-imaging module (Olympus BH2-UMA), which used a laser beam (λ = 532 nm), with a laser power of 2 mW, non filter was used. For calibration purposes, a Si wafer disc (521 cm^{-1}) was used. The vibrational range was from 100 to 3500 cm^{-1}. Raman peaks were identified using the RRUFF database (Lafuente et al., 2015), as well as

the information presented by Mycroft et al. (1990), Sasaki et al. (1998), Toniazzo et al. (1999), Frost et al. (2001 and 2004), Socrates (2004), Chio et al. (2005 and 2010), Chernyshova et al. (2007), and Jehlička et al. (2009).

2.5. Electrochemical techniques

For electrochemical measurements, a potentiostat-galvanostat (Bio-Logic™, VMP3 model) equipped with data logging (EC-Lab *version* 9.98), coupled to a 20A-20 V power supply (Bio-Logic™) was used.

OCP was measured by dipping the electrodes into 0 K medium and monitored for 60 min or until the potential values were stabilized. The stabilization of OCP was necessary in order to apply techniques, such as cyclic voltammetry (CV).

CV was conducted in both positive and negative scan directions, starting in the OCP, in a potential window of −0.46 to 1.04 V, at $\upsilon = 20\ mV\ s^{-1}$ scan rate. This technique was used to characterize the reactivity of chemical species present at the interfaces of each pyrite electrode after interaction with 0 K medium during 14 h. To calculate the degree of passivation of each electrode, the voltammetric charge (Q), defined as by $\int_{E_1}^{E_2} I(E)dE$ (Saavedra et al., 2018) was obtained by integration of the current peak in cyclic voltammograms obtained when the potential scan was initiated in positive direction.

2.6. Microorganism and culture medium

Leptospirillum sp. was used throughout this study, isolated and identified in previously published work (Casas-Flores et al., 2015). The cells were cultured in 9 K medium (Kim et al., 2002) containing 9 gL^{-1} Fe^{2+}, and supplemented with (gL^{-1}): KCl, 1; $MgSO_4.7H_2O$, 0.2; $(NH_4)H_2PO_4$, 2.6; and $FeSO_4{\cdot}7H_2O$, 44. pH was adjusted to 1.8 with H_2SO_4 10 N.

2.7. Bacterial attachment experiments

Bacteria were harvested at exponential phase by using centrifugation (10,000 rpm, 10 min), followed by a resuspension using 0 K media, in order to remove most of the iron present in the original media. The process was repeated until no iron was detected in the resuspension media, as measured by using the 1,10-phenantroline method. The concentrated and washed *Leptospirillum* sp. culture was measured by using a Neubauer chamber, being 4.2×10^{12} cell mL^{-1} the cellular concentration.

A Tait type electrochemical cell (50 mL) was used to evaluate the bacteria adherence over the mineral-made electrodes. Individual electrodes were submerged in 0 K media, and after 24 h were inoculated with a given final bacterial concentration. After 2 h, 100 µL aliquots were removed and planktonic cells counted (Neubauer chamber). Electrode attached cells were calculated as the difference between the inoculated and planktonic cells. Five cellular concentrations were assayed for each surface modified pyrite electrodes (2.2×10^8, 1.1×10^8, 2.2×10^7, 1.1×10^7 and 2.2×10^6 cell mL^{-1}).

3. Results and discussion

3.1. Open Circuit Potential (OCP) Profile

To evaluate stability of modified pyrite surfaces in 0 K medium, the OCP was monitored during 14 h of immersion (Fig. 1). From the moment of their immersion in the culture medium, the studied FeS_2 electrodes exhibited positive and negative shifts of OCP of different magnitudes, indicating the presence of oxidation and reduction processes associated with the interaction between the electrode and the culture medium.

The OCP of FeS_2 electrode shows a positive shift of 10 mV, being stabilized at ~0.56 V (Fig. 1, i) at relatively short times; this potential is similar to that reported in an acidic medium, 0.55 to 0.65 V (Hiskey and Pritzker, 1988). The slight, positive shift could be due to the pyrite surface oxidation by oxygen in the solution (Ahlberg et al., 1990), or to the formation of hydroxide coating (Moslemi et al., 2011). In the case of pyrite previously modified by ferric oxidation ($FeS_2/Fe(OH)_n,S^0$), the OCP exhibits a significant negative shift of slow stabilization at ~0.43 V (Fig. 1, ii). This modification indicates high reactivity towards reduction of species present at the $FeS_2/Fe(OH)_n,S^0$ surface, possibly due to reduction of oxidized compounds formed in the prior weathering. However, the OCP of the oxidized pyrite washed with methanol ($FeS_2/Fe(OH)_n$) shows a positive shift from 0.50 V, being stabilized at ~0.58 V (Fig. 1, iii), which evidences oxidative changes at the modified pyrite surface. Finally, the OCP of pyrite washed with hydrochloric acid (FeS_2/S^0) shows a negative shift of 0.35 V, being stabilized at ~0.29 V (Fig. 1, iv), the lowest OCP recorded so far.

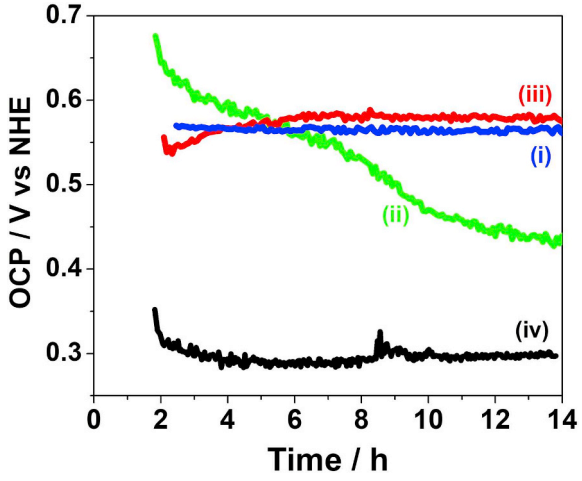

Fig. 1. OCP variation of pyrite electrodes (i) and modified pyrite electrodes over the time of immersion in 0 K culture medium: (ii) $FeS_2/Fe(OH)_n$, S^0; (iii) $FeS_2/Fe(OH)_n$ and (iv) FeS_2/S^0.

According to the OCP results, after 14 h immersed in 0 K, shifts towards potentials less positive than OCP appeared in modified pyrites and those with surface ($FeS_2/Fe(OH)_n,S^0$ and FeS_2,S^0), whereas shifts towards more positive potentials were present in pyrite and the one modified by ferric oxidation.

Interactions between mineral surfaces and the culture medium, qualitatively proposed by the OCP variation, are supported by the results obtained from spectroscopic and electrochemical characterizations of these surfaces (see below).

3.2. Raman Spectroscopy

Pyrite and surface modified pyrite electrodes remained immersed in 0 K culture medium for 48 h to ensure the electrode stability after weathering; however chemical stabilization of the different modified pyrite surface electrodes were corroborated by following the OCP potential in time, showing that after 14 h the OCP potentials remains nearly constant. Moreover EIS experiments were performed at different immersion time with all modified pyrite surfaces; the corresponding Kramer-Kroning test (Schönleber et al., 2014) confirm that the systems after 14 h remains in a stationary (see Supplementary Information, Fig. S2).

The FeS_2 electrode exhibited the characteristic peaks of this mineral (Fig. 2, i; Lafuente et al., 2015); however, pyrite electrodes with modified surfaces showed the presence of iron oxides (247–249, 298, 302, 412, 612, 615, 690 cm^{-1}) and Fe(II) hexahydrate, $[Fe(H_2O)_6]^{2+}$ (375 cm^{-1}) (Chio et al., 2005; Chernyshova et al., 2007). The presence of sulfates is also suggested by a peak at 983 cm^{-1} (Frost et al., 2004).

The pyrite electrode subjected to ferric oxidation ($FeS_2/Fe(OH)_n,S^0$)

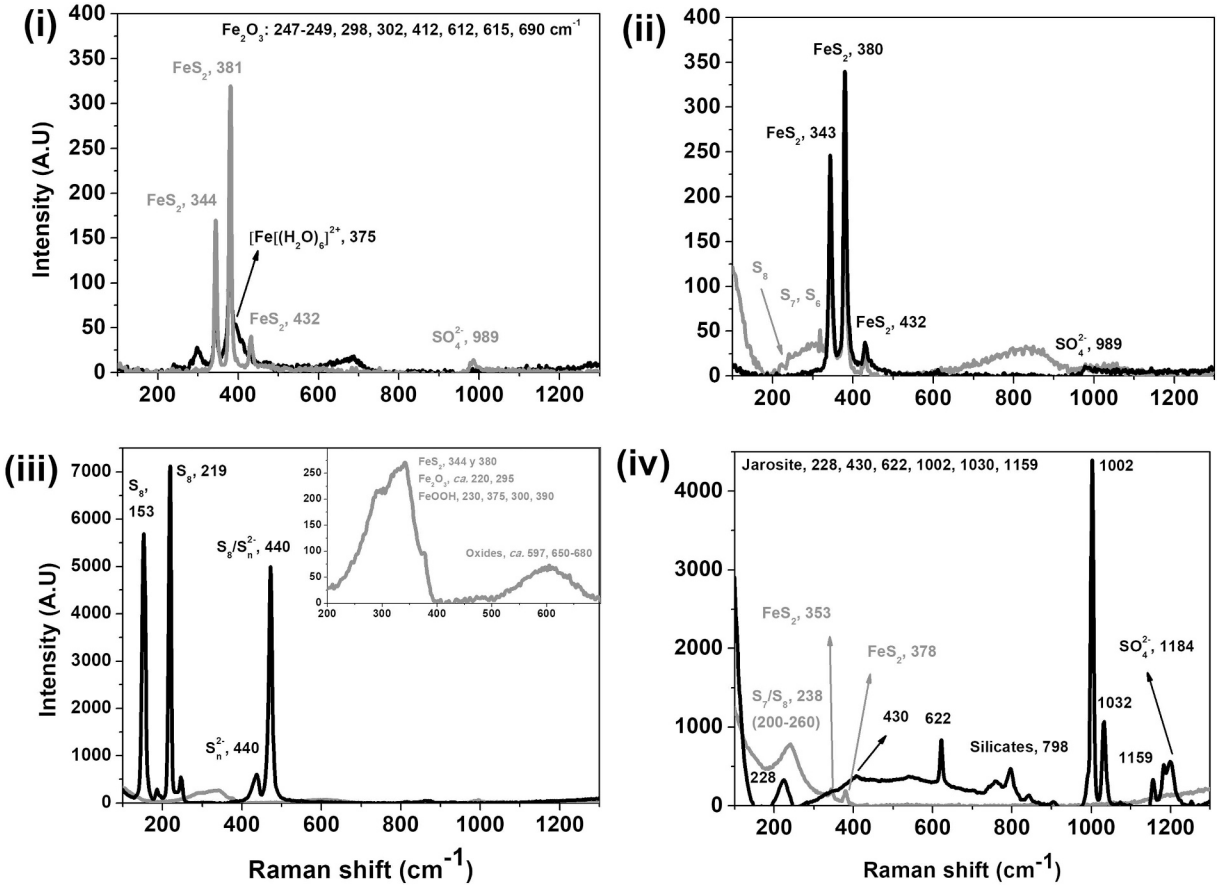

Fig. 2. Raman spectra of pyrite (i) and surface modified pyrite electrodes (ii to iv) before (0 h) and 48 h after immersion in 0 K medium. The electrodes are: (i) FeS_2; (ii) FeS_2/Fe(OH)n,S^0; (iii) FeS_2/Fe(OH)n and (iv) FeS_2/S^0. The same color code was used for peaks associated to chemical species at 0 h (gray) and 48 h (black).

before its exposure to 0 K medium (0 h), clearly displays three well-defined peaks corresponding to pyrite (343, 380 and 432 cm^{-1}; Mycroft et al., 1990; Toniazzo et al., 1999; Lafuente et al., 2015) and a region from 220 to 320 cm^{-1} of sulfur as S_8, S_7 and S_6 (Bondarenko and Gorbaty, 1997) (Fig. 2, ii). Also, an amorphous region between 670 and 860 cm^{-1} which may be related to silicates (e.g., nacrite), but rather corresponds to iron oxides such as maghemite (γ-Fe_2O_3) (Chernyshova et al., 2007). After chemical modification, this electrode exhibited magnetism.

Before it immersion in 0 K medium (0 h), the pyrite electrode subjected to ferric oxidation and methanol wash (FeS_2/Fe$(OH)_n$) exhibited two broad, noisy, regions at 210–400 and 500–700 cm^{-1} (Fig. 2, iii), which suggested the presence of FeS_2 (344, 380 cm^{-1}), Fe-oxides as Fe_2O_3 (ca. 220, 295, ca. 597, 650–680 cm^{-1}) and Fe-oxyhydroxides as goethite (230, 375, 300 and 390 cm^{-1}) (Chio et al., 2005; Chio et al., 2010; Chernyshova et al., 2007; Lafuente et al., 2015); the presence of sulfates is also suggested at 430–650 cm^{-1} (Frost et al., 2001 and 2004). Such regions were not detected after 48 h of immersion in 0 K medium; after this time, only Raman peaks associated to elemental sulfur and polysulfides were identified.

Finally, the pyrite electrode modified by ferric oxidation and subsequently washed with HCl (FeS_2/S^0) clearly exhibited pyrite peaks (353, 358 cm^{-1}) and a region from 200 to 320 cm^{-1} of S_8, S_7 and S_6 (Bondarenko and Gorbaty, 1997) (Fig. 2, iv). After 48 h, this electrode mainly showed peaks associated to jarosite on its surface (228, 430, 622 1002, 1030 and 1159 cm^{-1}) (Lafuente et al., 2015).

The presence of a greater proportion of iron related compounds in FeS_2/Fe$(OH)_n$, sulfides in FeS_2/S^0, and iron and sulfides in FeS_2/Fe $(OH)_n$,S^0 also corroborates the chemical modification underwent by the pyrite electrode.

Once the modification of pyrite electrodes had been corroborated, the electrodes were immersed in 0 K medium for 48 h to characterize the changes caused by the medium (weathering). According to the OCP profile obtained during the immersion time (Fig. 1), significant chemical modifications occurred at the surfaces of all electrodes during weathering. These chemical modifications are associated with iron oxidation by oxygen and interfacial changes of pH (Bonnissel-Gissinger et al., 1998), as well as with the interaction of the surface chemical species with the components of the culture medium (Lara et al., 2015).

The aforementioned chemical species were particularly identified on the FeS_2 electrode (Fig. 2, i) 48 h after its weathering in 0 K medium. They are associated with "scarce" oxidations, as was corroborated by a very slight increase in OCP, described in Fig. 1, which may be due to formation of oxides and sulfates (very low intensity regions < 50 U.A., with a maximum of 690 cm^{-1}) at the mineral surface resulting from the oxidative activity of 0 K medium. This result is important, because the formation of oxides and sulfates can modify significantly the reactivity and bacteria-mineral interaction.

The FeS_2/Fe$(OH)_n$,S^0 electrode (Fig. 2, ii), which showed reductive processes of the most negative OCP shift (Fig. 1) after 48 h of immersion in 0 K medium, exhibited mainly pyrite related peaks, possibly due to the solubilization of chemical species formed as HS^-.

For FeS_2/Fe$(OH)_n$ electrode (Fig. 2, iii) after 48 h weathering, higher-intensity peaks of ~~S^0~~ S_8 and S_n^{2-} were recorded. The formation of polysulfides and elemental sulfur can be due to activation of mineral corrosion processes because of the presence of iron (López-Cázares et al., 2017). The passive compounds formed at short times (0–48 h) for the FeS_2/S^0 electrode (Fig. 2, iv) are associated with high-intensity

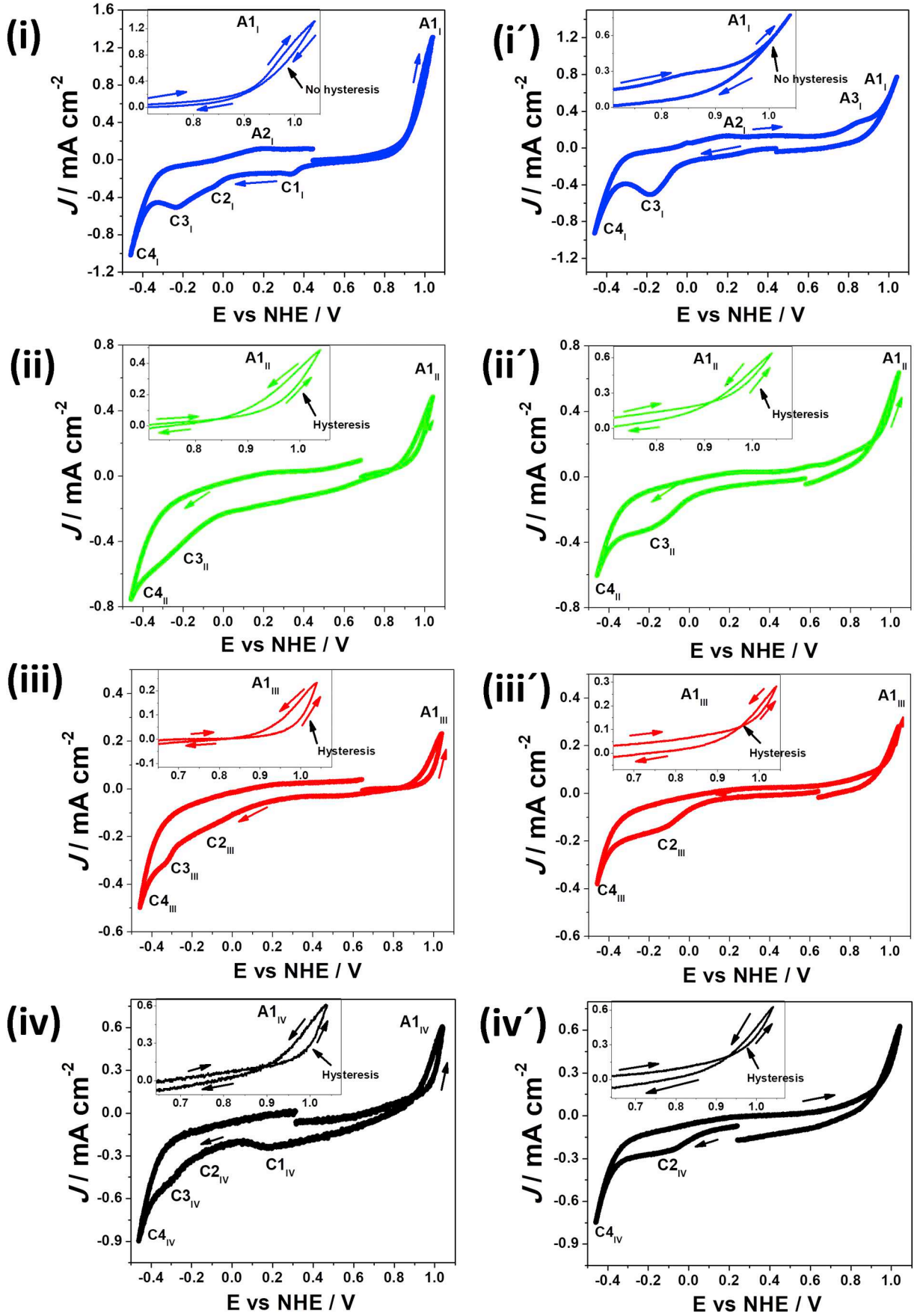

Fig. 3. Typical cyclic voltammograms (v = 20 mVs^{-1}) where the potential scan was initiated from OCP in the positive (i, ii, iii, iv) and negative (i´, ii´, iii´, iv´) directions. (i, i´) FeS_2; (ii, ii´) $FeS_2/Fe(OH)_n,S^0$; (iii, iii´) $FeS_2/Fe(OH)_n$; (iv, iv´) FeS_2/S^0. The electrodes were immersed during 14 h in 0 K medium, then the CVs were made.

peaks, corresponding to jarosite (Fig. S3) and sulphate.

3.3. Voltammetric study

Different chemical species present at the surface of pyrite electrodes studied herein, modify the reactivity of the mineral surface in 0 K culture medium. A voltammetric study was performed to evaluate this modification. Fig. 3 shows the voltammetric response for pyrite (Fig. 3, i) and modified pyrite electrodes: FeS_2/Fe(OH)$_n$,S^0 (Fig. 3, ii), FeS_2/Fe(OH)$_n$ (Fig. 3, iii) and FeS_2/S^0 (Fig. 3, iv), after 14 h of immersion in culture medium.

When the scan potential is initiated in the positive direction for FeS_2 (Fig. 3, i), one important oxidation process beginning at ~0.83 V ($A1_I$) is observed. On the reverse scan, several reduction processes take place. The first cathodic peak, $C1_I$, appears at 0.33 V, while three cathodic peaks, $C2_I$, $C3_I$ and $C4_I$, become visible at more negative potentials (between −0.04, −0.23 and − 0.36 V). Finally, when the scan potential is reversed, one anodic peak ($A2_I$) appears. The last three cathodic and anodic peaks ($A2_I$) are also observed when the scan potential is initiated in the negative direction (Fig. 3, i). However, when the scan potential is reversed, a new anodic peak ($A3_I$) emerges at 0.76 V, and the current associated with peak A1 is lower than that obtained in the positive scan direction (Fig. 3, i), whereas the peak C1 is not detected. In this way, anodic peak A1 is related to pyrite oxidation and the cathodic peaks $C2_I$, $C3_I$ and $C4_I$ are related reduction of oxidized compounds present on pyrite surface.

The pyrite electrochemical behavior in culture media is complex and a thorough study is needed to establish the electrochemical transformation taking place. These studies (electrochemical and Raman surface characterizations) were previously performed by our research team (Lara et al., 2015; Urbano et al., 2008) and the electrochemical reactions proposed in this manuscript are taken from those references.

The anodic process $A1_I$ exhibits a sudden increase in the current, attributed to pyrite oxidation and formation of S^0 according to Eqs. (1) and (2) (modified from Lara et al., 2015), proposed taking into consideration predominant chemical species based on their pKa and the pH of the culture medium.

$$FeS_{2(s)} + H_2PO_4^- + 4H_2O \rightleftharpoons FePO_{4(S)} + S^0_{(s)} + HSO_4^- + 9H^+ + 9e^- \quad (1)$$

E^0 = 0.369 V vs NHE (0.125 V vs SCE in Kelsall et al., 1999)

$$S^0_{(s)} + 4H_2O \rightleftharpoons HSO_4^- + 7H^+ + 6e^- \quad (2)$$

Besides, the reduction peak $C1_I$, observed only if the pyrite is previously oxidized, has been related to the reduction of iron hydroxides formed on the mineral surface during the pyrite oxidation, according to the following reaction (Eq. (3)) (Urbano et al., 2008).

$$FeOOH_{(s)} + 3H^+ + e^- \rightleftharpoons Fe^{2+} + 2H_2O \quad (3)$$

E^0 = −0.093 V vs NHE (Bard et al., 1980).

In the reduction peak, $C2_I$, pyrite can be transformed to H_2S and Fe^{2+} (Eghbalnia and Dixon, 2013). Alternately, this peak can also be attributed to the reduction of sulfur (Eqs. 4 and 5) (Hamilton and Woods, 1981).

$$FeS_{2(s)} + 4H^+ + 2e^- \rightleftharpoons Fe^{2+} + 2H_2S \quad (4)$$

E^0 = −0.093 V vs NHE (Kelsall et al., 1999)

$$S^0 + 2H^+ + 2e^- \rightleftharpoons H_2S \quad (5)$$

E^0 = 0.141 V vs NHE (Bard et al., 1980).

The reduction processes, $C3_I$ and $C4_I$, are identified by some authors as the reduction of sulfur phases formed during the initial pyrite reduction (i.e. FeS and metal-deficient sulfide) (Eqs. 6, 7 and 8; modified from Urbano et al., 2008).

$$FeS_{2(s)} + 2H^+ + 2e^- \rightleftharpoons FeS_{(s)} + H_2S \quad (6)$$

E^0 = −0.284 V vs NHE (Kelsall et al., 1999)

$$FeS_{(s)} + 2H^+ + 2e^- \rightleftharpoons Fe^0 + H_2S \quad (7)$$

$$FeS_{(s)} + 2H_2O \rightleftharpoons Fe(OH)_{2(s)} + H_2S \quad (8)$$

On the other hand, $A2_I$ is attributed to the oxidation of the H_2S generated at $C3_I$ and $C4_I$ via reactions in (Eqs. 6,7,8) (Liu et al., 2011). The oxidation peak $A3_I$ corresponds to the reaction described by Lara et al. (2015), who proposed the formation active component, $Fe_{1-t}S_{2-y(x)}$ and a passive component, $FePO_{4(S)}$ (Eqs. (9), (10) and (11)). The formation of iron deficient sulfur compounds (non-stoichiometric) have been demonstrated by several authors (Karthe et al., 1993, Mycroft et al., 1990, Bonnissel-Gissinger et al., 1998.

$$FeS_{2(s)} + 1.5yH_2O \rightleftharpoons Fe_{1-t}S_{2-y} + tFe^{2+} + 0.5yS^0_{(S)} + 0.5yS_2O_3^{2-} + 3yH^+ + 2(t + y)e^- \quad (9)$$

$$tFe^{2+} + tPO_4^{3-} \rightleftharpoons tFePO_{4(S)} + te^- \quad (10)$$

$$S_2O_3^{2-} + 5H_2O \rightleftharpoons 2SO_4^{2-} + 10H^+ + 8e^- \quad (11)$$

E^0 = 0.453 vs NHE (Bard et al., 1985).

However, the voltammograms of modified pyrite electrodes, FeS_2/Fe(OH)$_n$,S^0 (Fig. 3, ii), FeS_2/Fe(OH)$_n$ (Fig. 3, iii) and FeS_2/S^0 (Fig. 3, iv), exhibit a similar behavior with less anodic and cathodic peaks, and lower currents than voltammograms of pyrite electrode. Upon calculating the charge associated with the oxidation processes $A1_I$, $A1_{II}$,$A1_{III}$ and $A1_{IV}$ (Fig. 4), the values of 94, 27, 24 and 10 μC cm^{-2} are obtained for FeS_2, FeS_2/Fe(OH)$_n$, S^0, FeS_2/S^0 and FeS_2/Fe(OH)$_n$, respectively. The decrease in the charge related to pyrite oxidation is possibly associated with some degree of passivation of the electrodes; this statement is corroborated by the fact that the oxidation peak shows a hysteresis and a crossing between the currents in direct and reverse potential scans, usually correlated with the passive layer breaking (Fig. 3). This phenomenon was observed for chalchopyrite, product of the formation of passivating films (Arce and Gonzalez, 2002), whose nature was described above (Fig. 2).

In the case of FeS_2/Fe(OH), S^0 (Fig. 3, ii), when the voltammogram is initiated in the positive direction, only the oxidation process $A1_{II}$ is seen, followed by cathodic processes $C3_{II}$ and $C4_{II}$; in the scan performed in the negative direction, the same processes are seen although associated with a lower current. The anodic and cathodic processes observed could indicate a limited oxidation and reduction activity of pyrite, possibly due to the presence of passivating species that were characterized by Raman spectroscopy (Fig. 2).

Regarding FeS_2/Fe(OH)$_n$ (Fig. 3, iii), when the scan is started in the

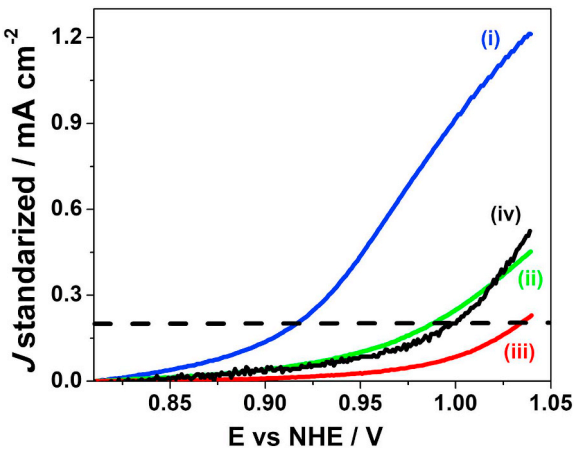

Fig. 4. Curves constructed from voltammetric data presented in Fig. 3, positive scans. Pyrite and surface modified pyrite electrodes after 14 h immersion in 0 K medium, (i) FeS_2; (ii) FeS_2/Fe(OH)$_n$,S^0; (iii) FeS_2/Fe(OH)$_n$; (iv) FeS_2/S^0.

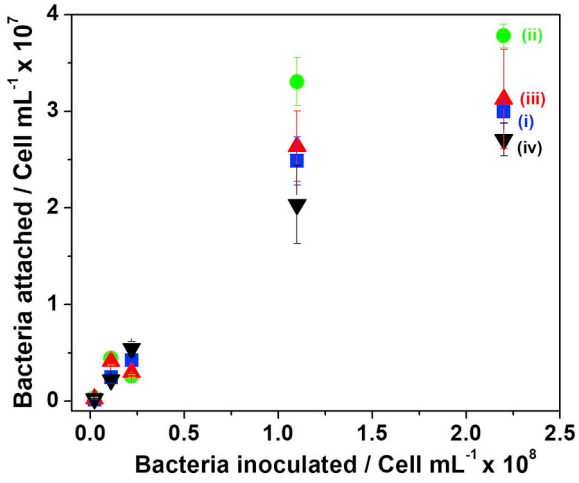

Fig. 5. Bacterial attachment experiments. Pyrite and surface modified pyrite electrodes were incubated in 0 K media, during 2 h, with different *Leptospirillum* sp. concentration. (i) FeS_2;(ii) $FeS_2/Fe(OH)_n$,S^0; (iii) $FeS_2/Fe(OH)_n$; (iv) FeS_2/S^0.

positive direction, the same oxidation process $A1_{III}$, though notably decreased, and reduction processes, $C1_{III}$, $C2_{III}$, $C3_{III}$ and $C4_{III}$ are observed. However, when it is initiated in the negative direction, only cathodic processes $C2_{III}$ and $C4_{III}$ are seen. The appearance of the peak $C2_{III}$ may indicate the reduction of elemental S^0, formed during the direct scan potential, and detected by Raman spectroscopy (Fig. 2), which also identified the presence of polysulfides on the surface of the mineral. The voltammogram for FeS_2/S^0 (Fig. 3, iv) exhibits the same peaks as $FeS_2/Fe(OH)_n$, and in addition, the reduction process $C1_{IV}$, which can be attributed to the reduction of iron hydroxides, also identified by Raman spectroscopy (Fig. 2).

To establish an additional quantitative measurement of the passivation phenomenon generated during immersion of modified pyrite surfaces in the culture medium, we have determined the potential necessary to achieve certain pyrite oxidation (selected current was 0.2 mA cm^{-2}). While the pyrite electrode requires a potential of 0.92 V, the surface modified pyrite electrodes require potentials of 0.98 V, 0.99 V and 1.04 V for $FeS_2/Fe(OH)_n$, S^0, FeS_2/S^0, $FeS_2/Fe(OH)_n$, respectively. These high potentials provoked the passive compounds detachment (Cruz et al., 2001). This indicates that the greater is the required potential, the more resistive is the passive layer exhibited by the electrode (Fig. 4). This strategy was also used to evaluate pyrite oxidation capacity, passivation condition, which, being associated with different minerals, forms galvanic interactions (Cruz et al., 1997; Cruz et al., 2001).

3.4. Bacterial attachment experiments

Fig. 5 shows a typical saturation behavior for pyrite and surface modified pyrite electrodes, indicating that all the available attachment places are occupied; similar behavior was observed in previously published work (Ohmura et al., 1993). Different attachment values were obtained for the different electrodes, presented here from higher to lower, as follow: (ii) $FeS_2/Fe(OH)_n$,S^0 (38 ± 3.2%); (iii) $FeS_2/Fe(OH)_n$ (31 ± 5.5%); (i) FeS_2 (27 ± 4.7%) and (iv) FeS_2/S^0 (18 ± 3.8%).

$FeS_2/Fe(OH)_n$,S^0 shows the higher attachment, in agreement with previous reports where the lixiviant bacteria preference of attachment over oxidized surfaces was demonstrated (López-Cázares et al., 2017). The process is possibly driven by a combination of physicochemical (charge, hydrophobicity, etc.), and biological interactions (chemotaxis, specific attachment proteins in the bacteria, etc.) between the bacteria and the mineral surface (Fang et al., 2000). Then, $FeS_2/Fe(OH)_n$ display a similar attachment even after intemperization, which show after this process a prevalence of sulfur associated compounds; similar results have been reported previously by other authors, where sulfur compounds were preferred as attachment places (Devasia and Natarajan, 2010; Devasia and Natarajan, 1996; Devasia et al., 1993). FeS_2 and especially FeS_2/S^0 presented lower attachment; the last one evolved during the intemperization process towards a surface mostly associated to iron related compounds (as jarosite), that probably affected the adherence process.

Moreover, our attachment values are relatively low when compared with previously published work, which in some experiments reported bacterial attachment values between 80 and 90% (Florian et al., 2011; Harneit et al., 2006). Probably this is related to the different set-ups, as we use massive fined-polished then chemically modified (#1200 grain) electrodes, and the aforementioned authors typically use grounded pyrite, in small 50–100 μm particles, so increasing the available interfacial area for bacteria-mineral interactions.

4. Conclusions

The interaction between the mineral and 0 K culture medium is crucial for the efficiency of solubilization of the metal of interest, particularly for mineral reactivity and its interaction with different elements participating in the bioleaching process (bacteria, culture medium, galvanic interactions, etc.).

This study reports the interaction of the abiotic culture medium, typically used in biohydrometallurgical processes, with pyrite and modified pyrite electrodes by mimicking different oxidation states of the mineral, without applying an external stimulus. The interaction between the culture medium and pyrite caused significant chemical changes to the mineral surface and formation of chemical species with passive behavior, such as elemental sulfur, polysulfides and jarosite (only on FeS_2/S^0). This passive behavior was shown in the electrochemical study, with a significant decrease in charge values associated with mineral oxidation processes. Chemical changes associated with weathering in the culture medium can be important during bacterial adhesion to mineral in biomining processes.

Acknowledgements

We want to acknowledge CONICET, Argentina and United Nations University-Biotechnology for Latinomerican and Caribbean (UNU-BIOLAC) for A. Saavedra's PhD scholarship and internship, respectively. Rosa Linda Tovar and Dr. Aurora Robledo (Metallurgy, UASLP) for DRX and Raman analyses, respectively; and Erasmo Mata-Martínez (Geology, UASLP) for mineral sample preparation.

Appendix A. Supplementary data

Supplementary data to this article can be found online at https://doi.org/10.1016/j.hydromet.2018.10.022.

References

Acevedo, F., Gentina, J.C., García, N., 1998. CO_2 supply in the biooxidation of an enargite-pyrite gold concentrate. Biotechnol. Lett. 20, 257–259.
Ahlberg, E., Forssberg, K.S.E., Wang, X., 1990. The surface oxidation of pyrite in alkaline solution. J. Appl. Electrochem. 20, 1033–1039.
Arce, E.M., Gonzalez, I., 2002. A comparative study of electrochemical behavior of chalcopyrite, chalcocite and bornite in sulfuric acid solution. Int. J. Miner. Process. 67, 17–28.
Bard, A.J., Faulkner, L.R., Leddy, J., Zoski, C.G., 1980. Electrochemical Methods: Fundamentals and Applications. Wiley, New York.
Bard, A.J., Parsons, R., Jordan, J., 1985. Standard Potentials in Aqueous Solution. IUPAC-Marcel Dekker Inc, New York.
Bondarenko, G., Gorbaty, Y.E., 1997. In situ Raman spectroscopic study of sulfur-saturated water at 1000 bar between 200 and 500°C. Geochim. Cosmochim. Acta 61, 1413–1420.
Bonnissel-Gissinger, P., Alnot, M., Ehrhardt, J.J., Behra, P., 1998. Surface oxidation of pyrite as a function of pH. Environ. Sci. Technol. 32, 2839–2845.

Casas-Flores, S., Gómez-Rodríguez, E.Y., García-Meza, J.V., 2015. Community of thermoacidophilic and arsenic resistant microorganisms isolated from a deep profile of mine heaps. AMB Express 5, 54.
Chernyshova, I.V., Hochella Jr, M.F., Madden, A.S., 2007. Size-dependent structural transformations of hematite nanoparticles. 1. Phase transition. Phys. Chem. Chem. Phys. 9, 1736–1750.
Chio, C.H., Sharma, S.K., Muenow, D.W., 2005. Micro-Raman studies of hydrous ferrous sulfates and jarosites. Spectrochim. Acta Part A Mol. Biomol. Spectrosc. 61, 2428–2433.
Chio, C.H., Sharma, S.K., Ming, L.C., Muenow, D.W., 2010. Raman spectroscopic investigation on Jarosite–Yavapaiite stability. Spectrochim. Acta Part A Mol. Biomol. Spectrosc. 75, 162–171.
Cruz, R., Lázaro, I., Rodríguez, J.M., Monroy, M., González, I., 1997. Surface characterization of arsenopyrite in acidic medium by triangular scan voltammetry on carbon paste electrodes. Hydrometallurgy 46, 303–319.
Cruz, R., Bertrand, V., Monroy, M., Gonzalez, I., 2001. Effect of sulfide impurities on the reactivity of pyrite and pyritic concentrates: a multi-tool approach. Appl. Geochem. 16, 803–819.
Cruz, R., Lázaro, I., González, I., Monroy, M., 2005. Acid dissolution influences bacterial attachment and oxidation of arsenopyrite. Miner. Eng. 18, 1024–1031.
Davis, G.B., Ritchie, A.I.M., 1986. A model of oxidation in pyritic mine wastes: part 1 equations and approximate solution. Appl. Math. Model. 10, 314–322.
Devasia, P., Natarajan, K., 1996. Role of bacterial growth conditions and adhesion in bioleaching of chalcopyrite by *Thiobacillus ferrooxidans*. Miner. Metall. Proc. 13, 82–86.
Devasia, P., Natarajan, K.A., 2010. Adhesion of *Acidithiobacillus ferrooxidans* to mineral surfaces. Int. J. Miner. Process. 94, 135–139.
Devasia, P., Natarajan, K.A., Sathyanarayana, D.N., Rao, G.R., 1993. Surface chemistry of *Thiobacillus ferrooxidans* relevant to adhesion on mineral surfaces. Appl. Environ. Microbiol. 59, 4051–4055.
Eghbalnia, M., Dixon, D.G., 2013. In situ electrochemical characterization of natural pyrite as a galvanic catalyst using single-particle microelectrode technique in ferric sulfate solutions. J. Solid State Electrochem. 17, 235–267.
Fang, H.H., Chan, K.Y., Xu, L.C., 2000. Quantification of bacterial adhesion forces using atomic force microscopy (AFM). J. Microbiol. Methods 40, 89–97.
Fernandez, M.G.M., Mustin, C., de Donato, P., Barres, O., Marion, P., Berthelin, J., 1995. Occurrences at mineral-bacteria interface during oxidation of arsenopyrite by *Thiobacillus ferrooxidans*. Biotechnol. Bioeng. 46, 13–21.
Florian, B., Noël, N., Thyssen, C., Felschau, I., Sand, W., 2011. Some quantitative data on bacterial attachment to pyrite. Miner. Eng. 24, 1132–1138.
Fredlein, R.A., Damjanovic, A., Bockris, J.O., 1971. Differential surface tension measurements at thin solid metal electrodes. Surf. Sci. 25, 261–264.
Frost, R.L., Fredericks, P.M., Kloprogge, J.T., Hope, G.A., 2001. Raman spectroscopy of kaolinites using different excitation wavelengths. J. Raman Spectrosc. 32, 657–663.
Frost, R.L., Kloprogge, J.T., Martens, W.N., 2004. Raman spectroscopy of the arsenates and sulphates of the tsumcorite mineral group. J. Raman Spectrosc. 35, 28–35.
Hamilton, I.C., Woods, R., 1981. An investigation of surface oxidation of pyrite and pyrrhotite by linear potential sweep voltammetry. J. Electroanal. Chem. Interfacial Electrochem. 118, 327–343.
Harneit, K., Göksel, A., Kock, D., Klock, J.H., Gehrke, T., Sand, W., 2006. Adhesion to metal sulfide surfaces by cells of *Acidithiobacillus ferrooxidans*, *Acidithiobacillus thiooxidans* and *Leptospirillum ferrooxidans*. Hydrometallurgy 83, 245–254.
Hiskey, J.B., Pritzker, M.D., 1988. Electrochemical behavior of pyrite in sulfuric acid solutions containing silver ions. J. Appl. Electrochem. 18, 484–490.
Jehlička, J., Vítek, P., Edwards, H.G.M., Hargreaves, M.D., Čapoun, T., 2009. Fast detection of sulphate minerals (gypsum, anglesite, baryte) by a portable Raman spectrometer. J. Raman Spectrosc. 40, 1082–1086.
Jones, C.A., Kelly, D.P., 2008. Growth of *Thiobacillus ferrooxidans* on ferrous iron in chemostat culture: influence of product and substrate inhibition. J. Chem. Technol. Biotechnol. Biotechnol. 33, 241–261.
Karthe, S., Szargan, R., Suoninen, E., 1993. Oxidation of pyrite surfaces: a photoelectron spectroscopic study. Appl. Surf. Sci. 72, 157–170.
Kelsall, G.H., Yin, Q., Vaughan, D.J., England, K.E.R., Brandon, N.P., 1999. Electrochemical oxidation of pyrite (FeS_2) in aqueous electrolytes. J. Electroanal. Chem. 471, 116–125.
Kim, T.W., Kim, C.J., Chang, Y.K., Ryu, H.W., Cho, K.S., 2002. Development of an optimal medium for continuous ferrous iron oxidation by immobilized *Acidithiobacillus ferrooxidans* cells. Biotechnol. Prog. 18, 752–759.
Lafuente, B., Downs, R.T., Yang, H., Stone, N., 2015. The Power of Databases: The RRUFF Project. In: Armbruster, T., Danisi, R.M. (Eds.), Highlights in Mineralogical Crystallography. W. De Gruyter, Berlin, pp. 1–30.
Lara, R.H., Vazquez-Arenas, J., Ramos-Sanchez, G., Galvan, M., Lartundo-Rojas, L., 2015. Experimental and theoretical analysis accounting for differences of pyrite and chalcopyrite oxidative behaviors for prospective environmental and bioleaching applications. J. Phys. Chem. C 119, 18364–18379.
Lázaro, I., Gonzalez, I., 1997. Electrochemical study of orpiment (As_2S_3) and realgar (As_2S_2) in acidic medium. J. Electrochem. Soc. 144, 4128.
Lázaro, I., Cruz, R., González, I., Monroy, M., 1997. Electrochemical oxidation of arsenopyrite in acidic media. Int. J. Miner. Process. 50, 63–75.
Liu, Y., Dang, Z., Wu, P., Lu, J., Shu, X., Zheng, L., 2011. Influence of ferric iron on the electrochemical behavior of pyrite. Ionics 17, 169–176.
López-Cázares, I., Patrón-Soberano, O., García-Meza, J.V., 2017. Bioelectrochemical changes during the early stages of chalcopyrite interaction with *Acidithiobacillus thiooxidans* and *Leptospirillum* sp. Fortschr. Mineral. 7, 156.
Marshall, K.C., 1986. Adsorption and adhesion processes in microbial growth at interfaces. Adv. Colloid Interf. Sci. 25, 59–86.
McGuire, M.M., Hamers, R.J., 2000. Extraction and quantitative analysis of elemental sulfur from sulfide mineral surfaces by high-performance liquid chromatography. Environ. Sci. Technol. 34, 4651–4655.
Moslemi, H., Shamsi, P., Habashi, F., 2011. Pyrite and pyrrhotite open circuit potentials study: Effects on flotation. Miner. Eng. 24, 1038–1045.
Murr, L.E., Brierly, J.M., 1978. The use of large-scale test facilities in studies of the role of microorganisms in commercial leaching operations. In: Murr, L.E., Torma, L.R., Brierley, J.M. (Eds.), Metallurgical Applications of Bacterial Leaching and Related Microbiological Phenomena. Elsevier, New York, pp. 491–520.
Mustin, J., Berthelin, P., De Donato, P., Marion, A., 1993. Surface Sulphur as promoting agent of pyrite leaching by *Thiobacillus ferrooxidans*. FEMS Microbial. 11, 7 l–78.
Mycroft, J.R., Bancroft, G.M., McIntyre, N.S., Lorimer, J.W., Hill, I.R., 1990. Detection of Sulphur and polysulphides on electrochemically oxidized pyrite surfaces by X-Ray photoelectron spectroscopy and Raman spectroscopy. J. Electroanal. Chem. Interfacial Electrochem. 292, 139–152.
Ohmura, N., Kitamura, K., Saiki, H., 1993. Selective adhesion of *Thiobacillus ferrooxidans* to pyrite. Appl. Environ. Microbiol. 59, 4044–4050.
Rohwerder, T., Gehrke, T., Kinzler, K., Sand, W., 2003. Bioleaching review part a. Appl. Microbiol. Biotechnol. 63, 239–248.
Saavedra, A., Figueredo, F., Cortón, E., Abrevaya, X.C., 2018. An electrochemical sensing approach for scouting microbial chemolithotrophic metabolisms. Bioelectrochemistry 123, 125–136.
Sasaki, K., Tsunekawa, M., Ohtsuka, T., Konno, H., 1998. The role of sulfur-oxidizing bacteria *Thiobacillus thiooxidans* in pyrite weathering. Colloids Surf. A Physicochem. Eng. Asp. 133, 269–278.
Schönleber, M., Klotz, D., Ivers-Tiffée, E., 2014. A method for improving the robustness of linear Kramers-Kronig validity tests. Electrochim. Acta 131, 20–27.
Socrates, G., 2004. Infrared and Raman Characteristic Group Frequencies: Tables and Charts. Wiley, New York.
Toniazzo, V., Mustin, C., Portal, J.M., Humbert, B., Benoit, R., Erre, R., 1999. Elemental sulfur at the pyrite surfaces: speciation and quantification. Appl. Surf. Sci. 143, 229–237.
Tuovinen, O.H., Kelly, D.P., 1973. Studies on the growth of *Thiobacillus ferrooxidans*. Arch. Mikrobiol. 88, 285–298.
Urbano, G., Reyes, V.E., Veloz, M.A., González, I., 2008. Pyrite − arsenopyrite galvanic interaction and electrochemical reactivity. J. Phys. Chem. C 112, 10453–10461.
Vera, M., Schippers, A., Sand, W., 2013. Progress in bioleaching: fundamentals and mechanisms of bacterial metal sulfide oxidation—part a. Appl. Microbiol. Biotechnol. 97, 7529–7541.
Watling, H.R., 2006. The bioleaching of sulphide minerals with emphasis on copper sulphides: a review. Hydrometallurgy 84, 81–108.
Xia, J., Yang, Y., He, H., Zhao, X., Liang, C., Zheng, L., Ma, C., Zhao, Y., Nie, Z., Qiu, G., 2010. Surface analysis of sulfur speciation on pyrite bioleached by extreme thermophile *Acidianus manzaensis* using Raman and XANES spectroscopy. Hydrometallurgy 100, 129–135.
Yang, Y., Harmer, S., Chen, M., 2015. Synchrotron-based XPS and NEXAFS study of surface chemical species during electrochemical oxidation of chalcopyrite. Hydrometallurgy 156, 89–98.
Zhang, S., Liu, W., 2017. Application of aerial image analysis for assessing particle size segregation in dump leaching. Hydrometallurgy 171, 99–105.